Journal of Physics: Conference Series **619** (2015) 012012 doi:10.1088/1742-6596/619/1/012012

# Anomalous Photoluminescence of Weakly Confined Excitons including Radiative Correction in Nano-to-Bulk Crossover Regime

**Takuya Matsuda, Nobuhiko Yokoshi, Hajime Ishihara**

Department of Physics and Electronics, Osaka Prefecture University, 1-1, Gakuen-cho, Naka-ku, Sakai, Osaka, 599-8531, Japan

E-mail: matsuda@pe.osakafu-u.ac.jp

**Abstract.** We develop a theoretical formalism to calculate photoluminescence (PL) spectrum of weakly confined excitons incorporating the microscopic nonlocal optical response. The nonlocality is caused by the center-of-mass (c. m.) motion of exciton and becomes remarkable in nano-to-bulk crossover regime. The theory successfully explains the characteristics of recently observed peculiar PL spectra in high quality CuCl films [5], wherein the signals appear at the exciton states with the very large radiative corrections not only for the lowest level but also for the higher ones including non-dipole types of excitons.

## 1. Introduction

The exciton-radiation coupling has attracted a great deal of interest from viewpoint of the remarkable sample size dependence [1-4]. If the c. m. wavefunctions of exciton coherently spread across the entire crystal with the size beyond the long-wavelength approximation (LWA), the spatial interplay between the exciton wave and light wave greatly affects the sample size dependence, so the nonlocal optical response plays an important role therein. Such a wave-wave interplay causes the large exciton-radiation interaction volume which leads to the anomalous optical response. For example, it has been theoretically predicted that the radiative decay becomes exceptionally fast with the increase of the sample size [5], and actually the experiment with the quite high quality CuCl films revealed that the observed radiative decay time reaches the order of 100 [fs] in degenerate four-wave mixing [6].

Recently, the above-mentioned anomalous aspects have also been found in the PL processes [7]. In a contrast of a standard picture of PL processes in solids, in the experiment in Ref. [7], it has been succeeded in systematically observing the PL signals from multiple exciton-radiation coupled modes in the high quality CuCl films with thickness of a few hundred nanometers. The observed PL spectra exhibit following unconventional aspects: (1) PL signals appear from multiple higher excited states. (2)The signals appear even from "optically forbidden" exciton states such as that with odd parity c. m. wavefunctions. (3)The signals appear at the energies of excitons including the remarkably large radiative corrections. The key to understand these features is the nonlocal wave-wave coupling established in the size beyond LWA that causes the extremely large exciton-radiation interaction volume. This leads to the ultrafast radiative decay of excitons even including non-dipole type states. In order to elucidate the PL processes

of wave-wave coupled system, the PL theory taking account of the microscopic nonlocal effect is necessary. The purpose of this paper is to develop such a theoretical formalism and demonstrate PL spectra which exhibit above-mentioned anomalous features.

## 2. Theory

We explain the calculation method of PL spectra for weakly confined excitons including radiative correction. We consider the whole Hamiltonian as $\hat{H} = \hat{H}_{\rm ex} + \hat{H}_{\rm rad} + \hat{H}_{\rm int} + \hat{H}_{\rm res} + \hat{H}_{\rm er}$, where $\hat{H}_{\rm ex}$, $\hat{H}_{\rm rad}$, $\hat{H}_{\rm int}$, $\hat{H}_{\rm res}$ and $\hat{H}_{\rm er}$ represent, respectively, the excitons, the radiation field, the interaction between excitons and radiation field, the reservoirs, and the interaction between excitons and reservoirs . From the whole Hamiltonian, we derive the Markovian master equation as $(\partial/\partial t)\hat{\rho}(t) = (1/{\rm i}\hbar)[\hat{H}_{\rm ex} + \hat{H}_{\rm rad} + \hat{H}_{\rm int},\ \hat{\rho}(t)] + \hat{\mathcal{L}}_{\rm damp}\hat{\rho}(t) + \hat{\mathcal{L}}_{\rm phase}\hat{\rho}(t)$, where $\hat{\mathcal{L}}_{\rm damp}\hat{\rho}(t) = \sum_\lambda \gamma_{\rm ex}^\lambda/2\big(2\hat{b}_\lambda\hat{\rho}(t)\hat{b}_\lambda^\dagger - \{\hat{b}_\lambda^\dagger\hat{b}_\lambda,\ \hat{\rho}(t)\}\big)$, $\hat{\mathcal{L}}_{\rm phase}\hat{\rho}(t) = \sum_\lambda \Gamma_{\rm ex}^\lambda/2\big[\hat{b}_\lambda^\dagger\hat{b}_\lambda\ [\hat{b}_\lambda^\dagger\hat{b}_\lambda\ \hat{\rho}(t)]\big]$. Here, $\hat{\rho}(t)$ is the density matrix, $\gamma_{\rm ex}^\lambda$, $\Gamma_{\rm ex}^\lambda$ and $\hat{b}_\lambda$, respectively, show the nonradiative decay rate, the dephasing rate and the annihilation operator of the $\lambda$th exciton state. From the master equation, we derive the motion equations of the $\lambda$th excitonic polarization $\langle\hat{b}_\lambda(t)\rangle$, the coherence between the $\lambda$th and $\lambda'$th exciton states $\langle\hat{C}_{\lambda,\lambda'}(t)\rangle = \langle\hat{b}_\lambda^\dagger(t)\hat{b}_{\lambda'}(t)\rangle$ $(\lambda \neq \lambda')$, and the $\lambda$th excitonic population $\langle\hat{N}_\lambda(t)\rangle = \langle\hat{b}_\lambda^\dagger(t)\hat{b}_\lambda(t)\rangle$ as

$$\frac{\partial}{\partial t}\langle\hat{b}_\lambda(t)\rangle = -\big({\rm i}\Omega_\lambda^{\rm ex} + \gamma_{\rm ex}^\lambda/2 + \Gamma_{\rm ex}^\lambda/2\big)\langle\hat{b}_\lambda(t)\rangle + \frac{\rm i}{\hbar}\int {\rm d}\boldsymbol{r}\ \boldsymbol{\mathcal{P}}_\lambda^*(\boldsymbol{r})\cdot\boldsymbol{E}(\boldsymbol{r},t), \tag{1}$$

$$\begin{aligned}\frac{\partial}{\partial t}\langle\hat{C}_{\lambda,\lambda'}(t)\rangle = &\Big[{\rm i}(\Omega_\lambda^{\rm ex} - \Omega_{\lambda'}^{\rm ex}) - \frac{\gamma_{\rm ex}^\lambda + \gamma_{\rm ex}^{\lambda'} + \Gamma_{\rm ex}^\lambda + \Gamma_{\rm ex}^{\lambda'}}{2}\Big]\langle\hat{C}_{\lambda,\lambda'}(t)\rangle \\ &+ \frac{\rm i}{\hbar}\int {\rm d}\boldsymbol{r}\ \boldsymbol{\mathcal{P}}_{\lambda'}^*(\boldsymbol{r})\cdot\boldsymbol{E}(\boldsymbol{r},t)\langle\hat{b}_\lambda^\dagger(t)\rangle - \frac{\rm i}{\hbar}\int {\rm d}\boldsymbol{r}\ \boldsymbol{\mathcal{P}}_\lambda(\boldsymbol{r})\cdot\boldsymbol{E}^*(\boldsymbol{r},t)\langle\hat{b}_{\lambda'}(t)\rangle\,,\end{aligned} \tag{2}$$

$$\begin{aligned}\frac{\partial}{\partial t}\langle\hat{N}_m(t)\rangle = &-\sum_{m(<\lambda)}\delta^{m,\lambda}\langle\hat{N}_\lambda(t)\rangle + \sum_{n(>\lambda)}\delta^{\lambda,n}\langle\hat{N}_n(t)\rangle - \gamma_{\rm ex}^\lambda\langle\hat{N}_\lambda(t)\rangle \\ &+ \frac{\rm i}{\hbar}\int {\rm d}\boldsymbol{r}\ \big(\boldsymbol{\mathcal{P}}_\lambda^*(\boldsymbol{r})\cdot\boldsymbol{E}(\boldsymbol{r},t)\langle\hat{b}_\lambda^\dagger(t)\rangle - \boldsymbol{\mathcal{P}}_\lambda(\boldsymbol{r})\cdot\boldsymbol{E}^*(\boldsymbol{r},t)\langle\hat{b}_\lambda(t)\rangle\big).\end{aligned} \tag{3}$$

Here, we introduce phenomenologically the level-to-level nonradiative decay rate $\delta^{\lambda,\lambda'}$ from $\lambda'$th exciton state to $\lambda$th exciton one into the motion equation of population Eq.(3), and $\boldsymbol{E}(\boldsymbol{r},t)$ is the classical Maxwell electric field. $\Omega_\lambda^{\rm ex}$ means the eigenfrequency of $\lambda$th exciton, and the expansion coefficient of the polarization $\boldsymbol{\mathcal{P}}_\lambda(\boldsymbol{r})$ is written as $\boldsymbol{\mathcal{P}}_\lambda(\boldsymbol{r}) = \boldsymbol{\mathcal{M}}\psi_\lambda(\boldsymbol{r})$. $\boldsymbol{\mathcal{M}}$ is the transition dipole moment and $\psi_\lambda(\boldsymbol{r})$ is proportional to the c. m. wavefunction of $\lambda$th exciton. Solving the motion equations Eqs.(1)-(3), and Maxwell's equation self-consistently, we can obtain the mean values of the polarization $\langle\hat{b}_\lambda\rangle$, the coherence $\langle\hat{C}_{\lambda,\lambda'}\rangle$, and the population $\langle\hat{N}_\lambda\rangle$ in the steady state. We calculate PL spectrum from the quantized output radiation field expressed in frequency component by using the photon Green function as $\hat{\boldsymbol{E}}_{\rm out}(\boldsymbol{r}_0,\omega) = \mu_0\omega^2\int {\rm d}\boldsymbol{r}'\ \mathbf{G}_{\rm out}(\boldsymbol{r}_0,\boldsymbol{r}',\omega)\cdot\hat{\boldsymbol{P}}_{\rm ex}(\boldsymbol{r}',\omega)$, where $\boldsymbol{r}_0$ is an arbitrary position outside the material. Here, under the rotating-wave approximation (RWA), the excitonic polarization operator $\hat{\boldsymbol{P}}_{\rm ex}(\boldsymbol{r},\omega)$ is represented in terms of the annihilation operator of excitons $\hat{b}_\lambda(\omega)$ in frequency component as $\hat{\boldsymbol{P}}_{\rm ex}(\boldsymbol{r},\omega) = \sum_\lambda \boldsymbol{\mathcal{P}}_\lambda(\boldsymbol{r})\hat{b}_\lambda(\omega)$. The photon Green function $\mathbf{G}_{\rm out}(\boldsymbol{r}_0,\boldsymbol{r}',\omega)$ includes information of the spatial structure of the background dielectric function, and thus, this formulation can be applied to an arbitrary sample shape. From the first-order correlation function, the spectrum is defined as $S(\boldsymbol{r}_0,\omega) \equiv \frac{1}{(2\pi)^2}\int_0^\infty {\rm d}t_1\int_0^\infty {\rm d}t_2\ {\rm e}^{{\rm i}\omega(t_2-t_1)}\ \langle\hat{\boldsymbol{E}}_{\rm out}^\dagger(\boldsymbol{r}_0,t_1)\cdot\hat{\boldsymbol{E}}_{\rm out}(\boldsymbol{r}_0,t_2)\rangle$.

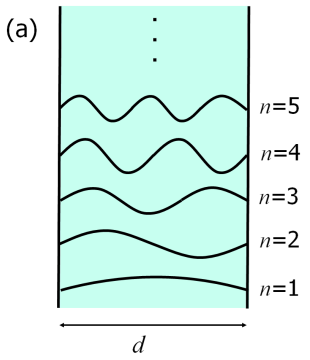


(b)

| $n$ | $\kappa_n$ [meV] |
|---|---|
| 1 | $\kappa_1$ = 1.12 |
| 2 | $\kappa_2$ = 3.10 |
| 3 | $\kappa_3$ = 6.60 |
| 4 | $\kappa_4$ = 55.6 |
| 5 | $\kappa_5$ = 3.29 |
| 6 | $\kappa_6$ = 0.635 |
| 7 | $\kappa_7$ = 0.215 |
| 8 | $\kappa_8$ = 0.100 |
| 9 | $\kappa_9$ = 0.052 |
| 10 | $\kappa_{10}$ = 0.033 |
| 11 | $\kappa_{11}$ = 0.019 |
| 12 | $\kappa_{12}$ = 0.015 |

**Figure 1.** (a) Sketch of the c. m. wavefunctions of confined excitons. (b)Table shows the radiative rates of the respective coupled modes.

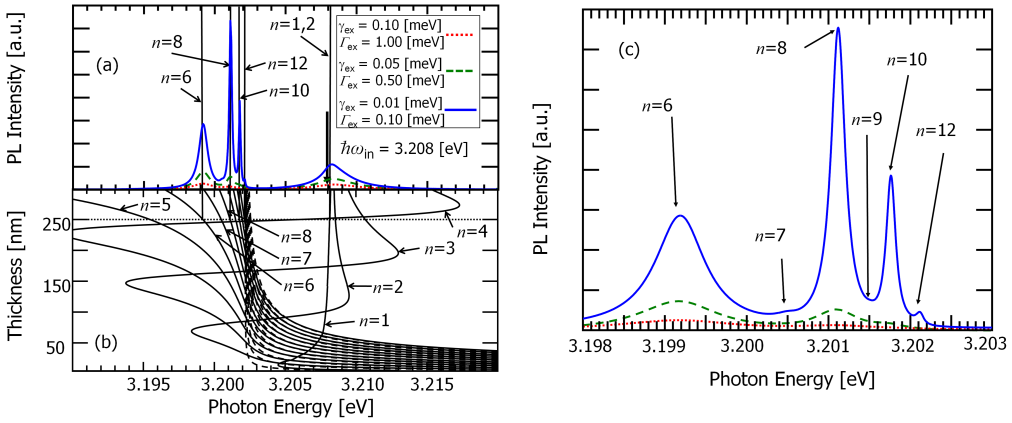


**Figure 2.** (a) Calculated PL spectra of a CuCl film with thickness of 250 [nm] for different values of nonradiative population decay rates. The assumed values of $\gamma_{\rm ex}$ and $\Gamma_{\rm ex}$ are indicated. The equal values of $\gamma_{\rm ex}$ and $\Gamma_{\rm ex}$, respectively, are taken for the different states. (b) The real parts of the eigenenergies of the coupled modes. Those for non-coupled excitons are also plotted by dashed lines. (c) An enlarged view of the spectra in Fig.2 (a) from 3.198 [eV] to 3.203 [eV].

## 3. Model and Results

In the numerical demonstrations, we consider a CuCl film with thickness $d$, where the c. m. motion is confined in the direction of the film thickness. With regard to the c. m. wavefunctions, we consider the simple sinusoidal waves without distortions near the surfaces as illustrated in Fig.1 (a). The excitation light is the monochromatic cw laser whose wavevector is perpendicular to the film surface. We divide the calculation process into the two steps. In the first step, we calculate the mean values of the polarization $\langle\hat{b}_\lambda\rangle$, the coherence $\langle\hat{C}_{\lambda,\lambda'}\rangle$, and the population $\langle\hat{N}_\lambda\rangle$ in the steady state in the presence of the incident light. In the second step, we cut off the incident light, and calculate PL spectrum by using the above mean values as initial ones. This procedure is valid in the presence of the sufficient excitonic dephasing that disconnects the initial coherent process from the incoherent emission one.

Figure 2 (a) shows calculated PL spectra, where we choose the thickness ($d$=250 [nm]) different from those in the experiment [7] for the sake of the clearer view of respective

contributions of the coupled modes, which does not change the essential features of observed PL spectra. The excitation light is assumed to be tuned to 3.208 [eV]. In Fig. 2 (c), we show an enlarged view of the spectra in Fig. 2 (a) from 3.198 [eV] to 3.203 [eV]. The table in Fig. 1 (b) shows the imaginary parts of the complex eigenenergies of exciton-radiation coupled modes corresponding to the radiative decay rates, and Fig. 2 (b) shows the real parts corresponding to the eigenenergies including radiative shifts. Those values can be obtained from the self-consistent solutions of Eq. (1) and the Maxwell's equations. In Fig. 2 (b), the eigenenergies of non-coupled excitons are also plotted (dashed line). Comparing the exciton-radiation coupled modes with the non-coupled excitons, we can see the large radiative shift and their drastic behavior with the change of the film thickness, where exciton states $m = 1, 2, \cdots$, in turn, changes from the lower branch modes to the upper branch ones with the increase of film thickness [5][8]. By comparing Fig.2 (a) with Fig.2 (b), we find that the respective peaks in PL spectrum appear at the eigenenergies of the coupled modes. In the experiment in Ref. [7], the observed PL signals for a CuCl film with the thickness of 325 [nm] are from the quantum states of $n$=1,2,3,4,7-12, where the even numbered states are optical forbidden if the LWA is satisfied because their wavefunctions have odd parity. The state $n$=5 is not detectable in the above experiment because its peak is too wide due to the very large radiative width. Our calculated result essentially reproduces similar features though the quantum states which appear in PL spectrum are slightly different owing to the different thickness. The remarkable point for this thickness is that the even numbered states (odd parity of states) clearly appear. This means that the parity of the light wave is odd like in the present case, and the selection rule is almost inverted from that under normal LWA. In this case, the states of $n$=4 has very large radiative width as seen in the table in Fig. 1(b), and hence, it is undetectable as $n$=5 in the experiment. The signals from the level of $n$=3 is not seen in Fig. 2(b) because its eigenenergy is higher than the excitation energy. The radiative decay rates of the levels of $n$=8-12 are of the order of 0.1 [meV]-0.01 [meV]. Therefore, the peaks of these states clearly appear when the nonradiative population decay rate $\gamma_{\rm ex}$ is smaller than them (blue solid line) in Fig. 2(a) and (c)). In the present case, we assume the level-to-level nonradiative decay rate smaller than the radiative decay rate of each quantum level. That is why their effect does not clearly appear in the present demonstration. The explicit effect of the level-to-level nonradiative decay will be studied in the next publication.

## 4. Summary

In summary, we develop a theoretical formalism to calculate PL spectra of weakly confined excitons beyond the LWA regime. By using this calculation method, we compute the PL spectra, and reproduce the essential features of the recent reported experimental results which show unconventional aspects: (1)The PL signals appear from multiple higher excited states. (2)The signals appear even from optically forbidden exciton states such as that with odd parity c. m. wavefunctions. (3)The signals appear at the energies of excitons with the radiative shifts. Although the quantitative comparison between the theory and experiment was not done because of the different incident conditions (The experiment was made under the pulse incidence), the study with more detailed comparison by further generalized theory would reveal the PL processes comprehensively for nano-to-bulk crossover regime, which is our future subject.

## References

[1] Takagahara T, 1987 Phys. Rev. B. **36** 9293
[2] Hanamura E, 1988 Phys. Rev. B. **37** 1273
[3] Gaponenko S V 1998 Optical Properties of Semiconductor Nanocrystals (Cambridge: Cambridge University)
[4] Ishihara H, J. Phys.: Condens. Matter **16** 2004 R247-R273
[5] Ishihara H, Kishimoto J, and Sugihara K, 2004 J. lumin. **108** 343-346
[6] Ichimiya M, Ashida M, Yasuda H, Ishihara, and H, Itoh T, 2009 Phys. Rev. Lett. **103** 257401
[7] Phuong L.Q, Ichimiya M, Ishihara H, Ashida M, 2012 Phys. Rev. B. **86** 235449